Smart Mater. Struct. **10** (2001) 300–304 www.iop.org/Journals/sm PII: S0964-1726(01)18316-3

Coupled extensional and torsional deformations of a piezoelectric cylinder

S Vidoli and R C Batra

Department of Engineering Science and Mechanics, MC 0219, Virginia Polytechnic Institute and State University, Blacksburg, Virginia 24061, USA

Received 30 May 2000, in final form 16 October 2000

Abstract
We derive a one-dimensional model from the three-dimensional equations to analyze electromechanical deformations of a piezoceramic cylinder. We show that its extensional and torsional deformations are coupled if the axis of polarization at a point makes a nonzero angle with the axis of the cylinder and the projection of the polarization vector on a cross section is perpendicular to the radial line through the point.

(Some figures in this article are in colour only in the electronic version; see www.iop.org)

1. Introduction

We study the electromechanical deformations of a piezoceramic cylinder with the axis of polarization $\boldsymbol{a}$, at a point making an angle $(\frac{1}{2}\pi - \alpha)$, with the axis of the cylinder, and the projection of $\boldsymbol{a}$ on a cross section is perpendicular to the radial line passing through the point. We focus on analyzing its coupled extensional and torsional deformations and first derive a one-dimensional model by using the principle of virtual work. From the assumed fields of the mechanical displacement and the electric potential, governing equations and constitutive relations are derived by integrating quantities over a cross section. The approach is similar to that of Mindlin [1]. Various attempts to systematically derive plate and rod theories have been reviewed by Koiter and Simmonds [2], Naghdi [3], Antman [4] and Leissa [5] amongst others. Vidoli and Batra [6] used a mixed variational principle of Yang and Batra [7] to derive equilibrium equations and constitutive relations for plate-like and rod-like piezoelectric bodies. Their approach considers the effects of double forces without moments which change the thickness of the plate and the cross section of the rod. The deformation field envisaged here is simpler than that considered in [6]. Consequently, the derived governing equations and the constitutive relations are easier to analyze. We study three problems, namely, the quasistatic deformations of a rod subjected to a uniform charge density along its length, quasistatic deformations of a rod fixed at one end and subjected to a torque at the other end, and traveling waves in the rod. The third problem exhibits the coupling between the speeds of the extensional and torsional waves for a large range of values of the angle α.

2. Formulation of the problem

We use rectangular Cartesian coordinates to describe the electromechanical deformations of a circular cylindrical body occupying the region $\mathcal{C} = S \times I$ in the stress-free reference configuration. Here S is a circle of inner radius R_1 and outer radius R_2 and I the real interval $[0, L]$. Thus R_2 is the outer radius of the cylinder and L its length. We assume that the origin of the coordinate system is at the center of the cross section $S \times \{0\}$ and the x_3-axis coincides with the centroidal axis of the cylinder. The position vector $\boldsymbol{x}$ of a point in $\mathcal{C}$ is given by

$$\boldsymbol{x} = \rho\cos\beta\boldsymbol{e}_1 + \rho\sin\beta\boldsymbol{e}_2 + z\boldsymbol{e}_3. \quad (1)$$

Here $\boldsymbol{e}_1$, $\boldsymbol{e}_2$ and $\boldsymbol{e}_3$ are, respectively, unit vectors along the x_1, x_2 and x_3 axes, ρ is the radius of the point, z its axial distance from the bottom end face of the cylinder, and β the angle between the x_1-axis and the projection of $\boldsymbol{x}$ onto the x_1–x_2 plane.

We assume that the body is made of a transversely isotropic piezoelectric material. However, the axis of transverse isotropy $\boldsymbol{a}$, which is the same as the material polarization vector, is not constant in $\mathcal{C}$ but varies according to the relation

$$\boldsymbol{a}(\rho, \beta, z) = -\cos\alpha\sin\beta\boldsymbol{e}_1 + \cos\alpha\cos\beta\boldsymbol{e}_2 + \sin\alpha\boldsymbol{e}_3 \quad (2)$$

where $\alpha \in [0, \frac{1}{2}\pi]$. For $\alpha = \frac{1}{2}\pi$, $\boldsymbol{a}$ is parallel to $\boldsymbol{e}_3$ and the piezoelectric body is homogeneous. However, for $\alpha \neq \frac{1}{2}\pi$, the projection of $\boldsymbol{a}$ onto the plane z = constant is along the tangent to the circle ρ = constant. For a fixed value of α, the angle between $\boldsymbol{a}$ and $\boldsymbol{e}_3$ is a constant; $\boldsymbol{a}$ does not vary along a radial line but changes as one moves in the circumferential direction. Since the material properties depend upon the vector $\boldsymbol{a}$, therefore, they are functions of the angular position, β, of a point and the body is nonhomogeneous.

The principle of virtual work for electromechanical deformations of a piezoelectric body is

$$\int_{\mathcal{C}} \left[(b_i - \rho\ddot{u}_i)\bar{u}_i + q\bar{\phi}\right] \mathrm{d}v = \int_{\mathcal{C}} \left[\sigma_{ij}e_{ij}(\bar{\boldsymbol{u}}) + D_i W_i(\bar{\phi})\right] \mathrm{d}v \quad (3)$$

where $\boldsymbol{u}$ is the mechanical displacement field, ϕ the electric potential, $\bar{\boldsymbol{u}}$ and $\bar{\phi}$ are virtual fields corresponding to $\boldsymbol{u}$ and ϕ, $\boldsymbol{b}$ and $\rho\ddot{\boldsymbol{u}}$ are the densities of the body and inertia forces, ρ is the mass density, a superimposed dot indicates differentiation with respect to time t, q is the density of body charges, $\boldsymbol{\sigma}$ is the stress tensor, $\boldsymbol{D}$ is the electric displacement, $e_{ij} = (u_{i,j} + u_{j,i})/2$ the infinitesimal strain tensor, $u_{i,j} = \partial u_i/\partial x_j$, $W_i = -\phi_{,i}$ the electric field, and a repeated index implies summation over the range of the index. The constitutive relations for the transversely isotropic piezoelectric body are

$$\begin{aligned}\sigma_{ij} &= \gamma_1 Q_{ik} e_{kl} Q_{lj} + \gamma_2 Q_{lk} e_{kl} Q_{ij} + \gamma_3 (P_{ik} e_{kj} + e_{ik} P_{kj}) \\ &\quad + \gamma_4 (e_{kk} P_{ij} + e_{kl} P_{lk} \delta_{ij}) + \gamma_5 (e_{kl} P_{lk}) P_{ij} \\ &\quad - \delta_1 (a_k W_k) Q_{ij} - \delta_2 (Q_{ik} W_k a_j + Q_{jk} W_k a_i)/2 \\ &\quad - \delta_3 (a_k W_k) P_{ij} \end{aligned} \tag{4}$$

$$\begin{aligned} D_i &= \nu_1 Q_{ij} W_j + \nu_2 P_{ij} W_j + \delta_1 Q_{ik} e_{kl} a_l + \delta_2 Q_{ik} e_{kl} a_l \\ &\quad + \delta_3 P_{ij} e_{jk} a_k \end{aligned} \tag{5}$$

where δ_{ij} is the Kronecker delta, $\gamma_1, \ldots, \gamma_5$ are the five elasticities of the transversely isotropic material, $\delta_1, \delta_2, \delta_3$ are the piezoelectric moduli, ν_1 and ν_2 are the dielectric constants, and $P_{ij} = a_i a_j$ and $Q_{ij} = \delta_{ij} - a_i a_j$ are respectively the projectors on the direction $\boldsymbol{a}$ of transverse isotropy and on the plane perpendicular to $\boldsymbol{a}$.

2.1. One-dimensional model

From the aforestated equations describing the three-dimensional deformations of the piezoelectric cylinder, we now derive a one-dimensional model in which the electric field is only axial and the mechanical deformations are extension and twisting of the cylinder. We presume that

$$u_i(\boldsymbol{x}, t) = w(z, t)\delta_{i3} + \theta(z, t)\varepsilon_{3ij} x_j \qquad \phi(\boldsymbol{x}, t) = \psi(z) \tag{6}$$

where ε_{ijk} is the permutation symbol or the alternating tensor, w the axial displacement and θ the angular twist of the cross section z = constant. The virtual electromechanical deformation field analogous to the deformations (6) is

$$\bar{u}_i(\boldsymbol{x}) = \bar{w}(z)\delta_{i3} + \bar{\theta}(z)\varepsilon_{3ij} x_j \qquad \phi(\boldsymbol{x}) = \bar{\psi}(z). \tag{7}$$

Substitution from equations (6) and (7) into equation (3) and recalling that $\bar{w}(z)$, $\bar{\theta}(z)$ and $\bar{\psi}(z)$ are arbitrary, we arrive at the following one-dimensional model:

$$N' + b = \rho A \ddot{w} \qquad T' + \mu = \rho J \ddot{\theta} \qquad \Delta' + \chi = 0 \tag{8}$$

where $N' = \mathrm{d}N/\mathrm{d}z$, and

$$\begin{aligned} N &= \int_S \sigma_{33}\,\mathrm{d}A \qquad & T &= \int_S \varepsilon_{3jk}\sigma_{3j} x_k\,\mathrm{d}A \\ \Delta &= \int_S D_3\,\mathrm{d}A \qquad & b &= \int_S b_3\,\mathrm{d}A \\ \mu &= \int_S \varepsilon_{3jk} b_j x_k\,\mathrm{d}A \qquad & \chi &= \int_S q\,\mathrm{d}A \end{aligned} \tag{9}$$

represent, respectively, the axial traction, the torque, the resultant axial electric displacement, the axial body force, the torsional moment due to the body forces, and the resultant charge per unit length of the cylinder. Furthermore, $A = \pi(R_2^2 - R_1^2)$ and $J = \pi(R_2^4 - R_1^4)/4$ equal, respectively, the area of cross section and the moment of inertia of the hollow circular cross section S. The boundary conditions involve the prescription at the end faces of either N or w, T or θ and Δ or ψ. Also, at time $t = 0$, w, $\dot{w}$, θ, and $\dot{\theta}$ need to be given.

We now substitute from (6) into (4) and (5), and the result into (3) to arrive at the following constitutive relations for the one-dimensional model

$$\begin{Bmatrix} N \\ T \\ \Delta \end{Bmatrix} = \begin{bmatrix} AK_{11} & BK_{12} & AK_{1e} \\ BK_{12} & JK_{22} & BK_{2e} \\ -AK_{1e} & -BK_{2e} & AK_{ee} \end{bmatrix} \begin{Bmatrix} w' \\ \theta' \\ \psi' \end{Bmatrix} \tag{10}$$

where

$$\begin{aligned} K_{11} &= \tfrac{1}{8}\big(3(\gamma_1 + \gamma_2 + \gamma_5) + 8(\gamma_3 + \gamma_4) \\ &\quad + (\gamma_1 + \gamma_2 + \gamma_5)\cos 4\alpha \\ &\quad + 4(\gamma_1 + \gamma_2 - 2\gamma_3 - 2\gamma_4 - \gamma_5)\cos 2\alpha\big) \\ K_{12} &= -\sin\alpha\cos\alpha\big(\gamma_1 + \gamma_2 - 2(\gamma_3 + \gamma_4) \\ &\quad - \gamma_5 + (\gamma_1 + \gamma_2 + \gamma_5)\cos 2\alpha\big) \\ K_{1e} &= -\frac{\sin\alpha}{2}\big(\delta_1 + \delta_2 + (\delta_1 + \delta_2 - \delta_3)\cos 2\alpha + \delta_3\big) \\ K_{22} &= \tfrac{1}{4}\big(\gamma_1 + \gamma_2 + 4\gamma_3 + \gamma_5 - (\gamma_1 + \gamma_2 + \gamma_5)\cos 4\alpha\big) \\ K_{2e} &= -\cos\alpha\big(\cos 2\alpha(\delta_1 + \delta_2 - \delta_3) + \delta_3 - \delta_1\big) \\ K_{ee} &= \tfrac{1}{2}\big(\nu_1 + \nu_2 + (\nu_1 - \nu_2)\cos 2\alpha\big) \\ B &= \frac{\pi(R_2^3 - R_1^3)}{3}. \end{aligned} \tag{11}$$

Equations (8) through (11) are also valid for a solid circular cylinder for which $R_1 = 0$.

3. Results for three problems

We study two static and one dynamic problem with the one-dimensional theory derived above and illustrate the interaction between extensional and torsional deformations.

3.1. Static problems

Consider a solid cylinder of length L and radius R fixed and grounded at the end $z = 0$, traction free and electrically insulated at the end $z = L$, and loaded only by a uniform charge of density $\bar{\chi}$ per unit length. This electric load can be applied by using a set of electric plates spanning the length of the cylinder. Thus $b = 0$, $\ddot{w} = 0$ and $\ddot{\theta} = 0$. The static electromechanical deformations of the cylindrical bar are governed by the differential equations

$$\begin{aligned} AK_{11}w'' + BK_{12}\theta'' + AK_{1e}\psi'' &= 0 \\ BK_{12}w'' + JK_{12}\theta'' + BK_{2e}\psi'' &= 0 \\ -AK_{1e}w'' - BK_{2e}\theta'' + AK_{ee}\psi'' + \bar{\chi} &= 0 \end{aligned} \tag{12}$$

and the boundary conditions

$$\begin{aligned} w = 0 \qquad \theta = 0 \qquad \psi &= 0 \text{ at } z = 0 \\ N = 0 \qquad T = 0 \qquad \Delta &= 0 \text{ at } z = L. \end{aligned} \tag{13}$$

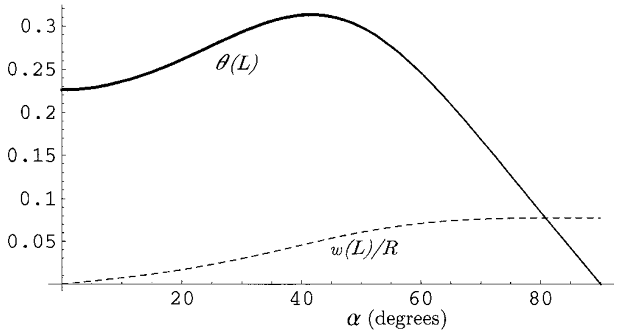

Figure 1. The variation with the angle α of the angular twist, $\theta(L)$, and the normalized extension, $w(L)/R$, of the end $z = L$ of a PZT5A cylindrical rod fixed at the end $z = 0$ and subjected to a uniform charge density along its length.

This boundary-value problem has the solution

$$w(z) = \frac{(AJK_{22}K_{1e} - B^2K_{12}K_{2e})}{AD}\frac{(2L-z)z}{2}\bar{\chi}$$

$$\theta(z) = \frac{B^2(K_{11}K_{2e} - K_{12}K_{1e})}{BD}\frac{(2L-z)z}{2}\bar{\chi}$$

$$\psi(z) = \frac{(B^2K_{12}^2 - AJK_{11}K_{22})}{AD}\frac{(2L-z)z}{2}\bar{\chi} \qquad (14)$$

where $D = AJK_{22}(K_{1e}^2 + K_{11}K_{ee}) - B^2(K_{11}K_{2e}^2 + K_{12}^2K_{ee})$. The angular twist $\theta(L)$ of the end $z = L$ of the cylinder and its normalized extension $w(L)/R$ against the angle α are plotted in figure 1 for a PZT5A solid cylinder of radius 2 mm and length 2 cm. Values of the material parameters for the PZT5A are listed below:

$$\gamma_1 = 45.2 \text{ GPa} \qquad \gamma_2 = 54 \text{ GPa} \qquad \gamma_3 = 42.2 \text{ GPa}$$

$$\gamma_4 = 50.8 \text{ GPa} \qquad \gamma_5 = -99.1 \text{ GPa}$$

$$\delta_1 = -7.21 \text{ C m}^{-2} \qquad \delta_2 = 12.32 \text{ C m}^{-2}$$

$$\delta_3 = 15.12 \text{ C m}^{-2}$$

$$\nu_1 = 1.53 \times 10^{-8} \text{ F m}^{-1} \qquad \nu_2 = 1.50 \times 10^{-8} \text{ F m}^{-1}.$$

Thus $(\gamma_1 + \gamma_2)/(2\gamma_3 + 2\gamma_4 + \gamma_5) \simeq 0.23$. Results plotted in figure 1 reveal that the normalized axial elongation attains its maximum value for $\alpha = \pi/2$, and the angular twist is maximum for $\alpha \simeq 42°$. Hence a PZT5A cylinder with the axis of polarization at each point making an angle of about 48° with the axis of the cylinder will exhibit maximum torsional deformations when subjected to a uniformly distributed charge along its length.

Consider the PZT5A solid cylinder studied above but assume that there are no body forces and distributed charges; i.e. $b = 0$, $\mu = 0$, $\chi = 0$ in equations (8). The cylinder is clamped and grounded at the end $z = 0$ and subjected only to the torque T_L at the end $z = L$. Thus

$$w(0) = 0 \qquad \theta(0) = 0 \qquad \psi(0) = 0$$

$$N(L) = 0 \qquad T(L) = T_L \qquad \Delta(L) = 0. \qquad (15)$$

The solution of equations (8) under the boundary conditions (15) is

$$N(z) = 0 \qquad T(z) = T_L \qquad \Delta(z) = 0. \qquad (16)$$

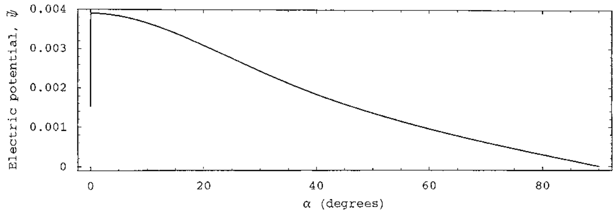

Figure 2. The variation with the angle α of the difference in the electric potential between the end faces of a PZT5A solid cylinder subjected to pure torques at the end faces.

We can solve constitutive relations (10) for w', θ' and ψ' in terms of T_L, and thus obtain the following expression for the electric potential, $\psi(L)$, at the end $z = L$:

$$\psi(L) = LT_L[(K_{12}^2 - K_{11}K_{2e})]/[B(K_{12}K_{1e}K_{2e} - K_{11}K_{2e}^2 + K_{12}^2(K_{2e} + K_{ee})) - AJK_{22}(K_{12}K_{1e} + K_{11}K_{ee})/B]. \qquad (17)$$

We have plotted in figure 2 the dependence upon the angle α of the non-dimensional electric potential, $\tilde{\psi}(L)$, defined as

$$\tilde{\psi}(L) = \frac{\psi(L)BL(\delta_1 + \delta_2 - \delta_3)}{T_L}. \qquad (18)$$

As expected, $\tilde{\psi}(L)$ is maximum for $\alpha \simeq 0$ and gradually decreases to zero for $\alpha = \pi/2$. Thus a PZT5A cylindrical disk with the polarization vector everywhere perpendicular to the radial line and perfectly bonded to another deformable body can be used to measure the torsional deformations of the surface to which it is perfectly bonded.

3.2. Dynamic problem

We now explore, in the absence of distributed charges and body forces, the dependence upon the angle α of the relative proportion of the torsional and extensional waves propagating along the hollow cylinder. From the governing equations:

$$AK_{11}w'' + BK_{12}\theta'' + AK_{1e}\psi'' = \rho A\ddot{w}$$

$$BK_{12}w'' + JK_{22}\theta'' + BK_{2e}\psi'' = \rho J\ddot{\theta}$$

$$AK_{1e}w'' + BK_{2e}\theta'' - AK_{ee}\psi'' = 0 \qquad (19)$$

we eliminate ψ, non-dimensionalize the variables through

$$\bar{w} = 2w/R_2 \qquad \bar{z} = 2z/R_2 \qquad \bar{t} = t(2/R_2)\sqrt{K_{11}/\rho} \qquad (20)$$

to obtain

$$\hat{K}_{11}w'' + \tfrac{2}{3}\hat{K}_{12}\theta'' = \ddot{w} \qquad \tfrac{2}{3}\hat{K}_{21}w'' + \hat{K}_{22}\theta'' = \ddot{\theta}. \qquad (21)$$

In equations (21), we have dropped the superimposed bar, the derivatives are with respect to non-dimensional variables, and

$$\hat{K}_{11} = \left(K_{11} + \frac{K_{1e}^2}{K_{ee}}\right)\Big/K_{11}$$

$$\hat{K}_{12} = \left(K_{12} + \frac{K_{1e}K_{2e}}{K_{ee}}\right)\Big/K_{11}$$

$$\hat{K}_{21} = K_{12}/K_{11} \qquad \hat{K}_{22} = \left(K_{22} + \frac{4K_{2e}^2}{9K_{ee}}\right)\Big/K_{11}. \qquad (22)$$

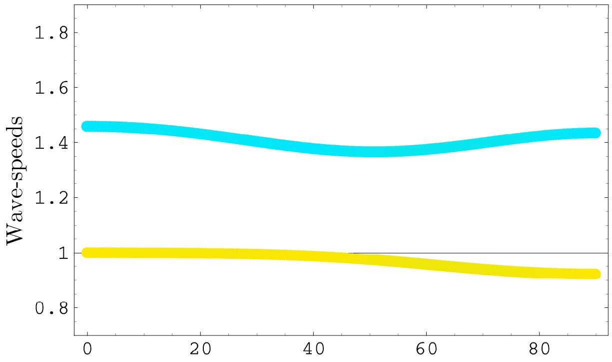

(*a*)

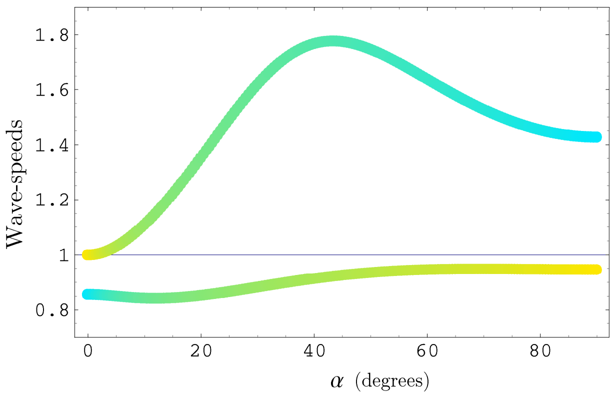

(*b*)

Figure 3. (*a*) The dependence upon the angle α of the extensional (yellow (or lower gray) curve) and torsional (blue (or upper dark) curve) wave speeds in a PZT5A cylinder. (*b*) The dependence upon the angle α of the extensional (yellow (or light gray) part of the curve) and torsional (blue (or black) part of the curve) wave speeds in a piezoceramic cylinder with moduli different from that of PZT5A. The green (or dark grey) part of the curve indicates the interaction between the two waves.

Table 1.

	$\alpha \to 0$	$\alpha \to \pi/2$
v_w^2	1	$\left(1 + \dfrac{\delta_3^2}{\nu_2(2\gamma_3 + 2\gamma_4 + \gamma_5)}\right)^{-1}$
v_θ^2	$\dfrac{\gamma_1 + \gamma_2}{\gamma_3}\left(1 + \dfrac{4\delta_2^2}{9\nu_1\gamma_3}\right)^{-1}$	$\dfrac{2(\gamma_3 + \gamma_4) + \gamma_5}{\gamma_3}$

We seek solutions of (21) in the form of traveling waves, i.e.

$$w = \hat{w}(z \pm vt) \qquad \theta = \hat{\theta}(z \pm vt) \tag{23}$$

where v is the non-dimensional wave speed. The speeds v_w and v_θ respectively of the extensional and torsional waves for $\alpha \to 0$ and $\alpha \to \pi/2$ are listed in table 1.

We note that usually

$$\frac{\delta_3^2}{\nu_2(2\gamma_3 + 2\gamma_4 + \gamma_5)} \ll 1 \qquad \text{and} \qquad \frac{4\delta_2^2}{9\nu_1\gamma_3} \ll 1. \tag{24}$$

Thus the speeds of extensional waves for $\alpha \to 0$ and $\alpha \to \pi/2$ are nearly the same. However, the speeds of the torsional waves for $\alpha \to 0$ and $\alpha \to \pi/2$ may be quite different because of the independent values of $(\gamma_1 + \gamma_2)$ and $(2\gamma_3 + 2\gamma_4 + \gamma_5)$; these are respectively proportional to the transverse and longitudinal Young's moduli of the material.

Figure 3(*a*) exhibits for the PZT5A solid cylinder the non-dimensional wave speeds as a function of the angle α. The yellow (lower gray) curve indicates an essentially extensional wave and the blue (upper dark) curve an essentially torsional wave. It is clear that there is hardly any interaction between the two waves; this is because for the PZT5A,

$$\frac{\gamma_1 + \gamma_2}{\gamma_3} = 2.35 \qquad \text{and} \qquad \frac{2(\gamma_3 + \gamma_4) + \gamma_5}{\gamma_3} = 2.06 \tag{25}$$

are close to each other and both are greater than one.

We have plotted in figure 3(*b*) the non-dimensional wave speeds for a cylinder made of a hypothetical material for which $\gamma_1 = 13.56$ GPa, $\gamma_2 = 16.2$ GPa, $\gamma_3 = 63.3$ GPa, and values of other material parameters are the same as those for the PZT5A. The green (or dark gray) part of the curve reflects the fact that for a large range of values of α, the speeds of torsional and extensional waves are comparable with each other. For these values of α, the extensional and torsional phenomena are strongly coupled.

4. Conclusions

We have deduced from the three-dimensional governing equations a one-dimensional model to describe the torsional and extensional deformations of a PZT cylinder. At every point of the cylinder the axis of transverse isotropy makes an angle of $(\frac{1}{2}\pi - \alpha)$ with the axis of the cylinder, and the projection of the axis of transverse isotropy on a cross section is normal to the radial line through the point. For the cylinder made of a PZT5A, the extensional and torsional wave speeds depend weakly upon the angle α and are quite different from each other. However, when the longitudinal and transverse Young's moduli of the material of the cylinder are quite different, there is a large range of values of α for which the extensional and torsional deformations of the cylinder are strongly coupled. A PZT5A cylinder with $\alpha \neq \pi/2$ and subjected to a uniformly distributed charge density along its length exhibits both torsional and extensional deformations; the former are maximum for $\alpha \simeq 42°$ and the latter for $\alpha = 90°$. Whereas for $\alpha \simeq 42°$ both torsional and extensional deformations occur, for $\alpha = 90°$ only extensional deformations are realized. For $\alpha \simeq 0°$, there is a measurable difference in the electric potential across the end faces of a circular cylindrical PZT5A disk subjected to pure torques at the end faces. Thus, such a disk can be used to gauge torsional deformations of the surface to which its one end face is perfectly bonded.

References

[1] Mindlin R D 1952 Forced thickness-shear and flexural vibrations of piezoelectric crystal plates *J. Appl. Phys.* **23** 83–8

[2] Koiter W T and Simmonds J G 1972 Foundations of shell theory *Proc. IUTAM Cong. (Moscow)* pp 150–76

[3] Naghdi P M 1972 The theory of shells and plates *Handbuch der Physik* vol VIa/2, ed C Truesdell (Berlin: Springer)

[4] Antman S S 1972 The theory of rods *Handbuch der Physik* vol VIa/2 (Berlin: Springer)

[5] Leissa A W 1987 Recent research in plate vibrations 1981–85 Part I: Classical theory *The Shock and Vibration Digest* **19** 11–18

Leissa A W 1987 Recent research in plate vibrations 1981–85 Part II: Complicating effects *The Shock and Vibration Digest* **19** 10–24

[6] Vidoli S and Batra R C 2000 Derivation of plate and rod equations for a piezoelectric body from a mixed three-dimensional variational principle *J. Elasticity* at press

[7] Yang J S and Batra R C 1995 Mixed variational principles in nonlinear piezoelectricity *Int. J. Nonlinear Mechs.* **3** 719–26